

Published in final edited form as:

ACS Nano. 2013 December 23; 7(12): 11129–11137. doi:10.1021/nn404853z.

Delivering Nanoparticles to Lungs While Avoiding Liver and Spleen through Adsorption on Red Blood Cells

Aaron C. Anselmo¹, Vivek Gupta^{1,2}, Blaine J. Zern³, Daniel Pan³, Michael Zakrewsky¹, Vladimir Muzykantov³, and Samir Mitragotri^{1,*}

¹Department of Chemical Engineering, Center for Bioengineering, University of California, Santa Barbara, CA 93106

³Department of Pharmacology and Center for Translational Targeted Therapeutics and Nanomedicine, Perelman School of Medicine, University of Pennsylvania

Abstract

Nanoparticulate drug delivery systems are one of the most widely investigated approaches for developing novel therapies for a variety of diseases. However, rapid clearance and poor targeting limit their clinical utility. Here, we describe an approach to harness the flexibility, circulation, and vascular mobility of red blood cells (RBCs) to simultaneously overcome these limitations (Cellular Hitchhiking). A non-covalent attachment of nanoparticles to RBCs simultaneously increases their level in blood over a 24 hour period and allows transient accumulation in the lungs, while, reducing their uptake by liver and spleen, RBC-adsorbed nanoparticles exhibited ~3-fold increase in blood persistence and ~7-fold higher accumulation in lungs. RBC-adsorbed nanoparticles improved lung/liver and lung/spleen nanoparticles accumulation by over 15-fold and 10-fold, respectively. Accumulation in lungs is attributed to mechanical transfer of particles from RBC surface to lung endothelium. Independent tracing both nanoparticles and RBCs in vivo confirmed that RBCs themselves do not accumulate in lungs. Attachment of anti-ICAM-1 antibody to the exposed surface of NPs that were attached to RBCs led to further increase in lung targeting and retention over 24 hours. Cellular hitchhiking onto RBCs provides a new platform for improving the blood pharmacokinetics and vascular delivery of nanoparticles while simultaneously avoiding uptake by liver and spleen, thus opening the door for new applications.

Keywords

hitchhiking; cell-mediated drug delivery; nanomedicine; nanotechnology

Nanoparticles (NPs) are actively explored for encapsulation and targeted delivery of drugs for improving the current treatment strategies for cancer and other diseases.^{1–3} Several preclinical studies have demonstrated the use of nanoparticles for targeting various cancers

^{*}To whom correspondence should be addressed: Prof. Samir Mitragotri, Department of Chemical Engineering, University of California, Santa Barbara, CA 93106, Ph: 805-893-7532, Fax: 805-893-4731, samir@engineering.ucsb.edu.

2 Current Address. School of Pharmacy, Keck Graduate Institute, 535 Watson Dr., Claremont, CA 91711

Supporting Information Available: Supporting SI Figures and captions. This material is available free of charge via the Internet at http://pubs.acs.org.

including breast, prostate and lung. $^{3-7}$ Some of these strategies have also advanced to clinical studies and have yielded promising early results. $^{8-11}$ Encapsulation in nanoparticles provides distinct advantages over free drugs including targeting and sustained release. $^{12, 13}$ Nanoparticles, however, suffer from the limitation of rapid clearance by the mononuclear phagocytic system (MPS) located primarily in the liver and spleen, thereby limiting the dose available for the disease site. $^{14-16}$

Several strategies have been proposed to address this limitation. The primary strategy includes grafting hydrophilic polymers such as polyethylene glycol (PEG) and poloxamer molecules on the nanoparticle surface to decrease MPS uptake. ^{17, 18} PEG serves to mitigate the interactions of nanoparticles with macrophages in the MPS, thereby reducing their immune clearance. However, PEG-modified nanoparticles have been shown to activate the immune system and lose efficacy upon repeated administrations. ^{19–21} Conjugation of CD47 or peptides derived from this self-recognition determinant to the surface of NP is an alternative approach. ²²

In theory, blood elements with a favorable circulation profile may be used as "natural carriers" improving the NP pharmacokinetics. For example, red blood cells (RBC) represent an attractive carrier for optimizing NP circulation and, perhaps, delivery to certain intravascular targets. ^{23–26} Preclinical studies in diverse animal species documented that coupling of drugs to RBC surface improves their delivery and therapeutic effects. ^{27–29} Coupling of NPs to RBCs has the potential to dramatically alter NP behavior in circulation. In addition, pharmacokinetics of RBC/NP complex may be more favorable than that of free NP in some medical settings. Here, we investigate this hypothesis and demonstrate that attachment to RBCs reduces NP uptake by the MPS organs (liver and spleen).

Results

Attachment of Nanoparticles

Spherical polystyrene nanoparticles (200nm or 500nm diameter) were attached to RBCs by incubation at varying particle:RBC ratios up to 100:1. Particle attachment to RBC was mediated by electrostatic and hydrophobic interactions. ^{23, 30, 31} The attachment was confirmed through SEM (Figs. 1a–b) and was quantified using ³H-radiolabeled nanoparticles (Fig. 1c). At a particle:RBC ratio of 100:1, RBCs on average carried ~24 particles (200nm) per cell (Fig. 1c). Under these conditions, >99% of RBCs carried at least 1 attached particle (SI Fig. 1). Attachment of particles did not induce RBC hemolysis (Fig. 1d).

Nanoparticles attached to RBCs did not detach from RBCs under static conditions (Fig. 2a). Yet the binding was reversible and particles detached from RBCs upon exposure to physiological shear stresses experienced by RBCs in circulation (5 Pa for 15 minutes at 37°C, Fig. 2b). In theory, this may enable a natural mechanism for release or transfer of NP load. Microscopic observations of RBCs supported this notion. Nanoparticle-laden RBCs were structurally fixed prior to exposure to shear and small indentations that matched the size of the particles were found. These indentations likely represent areas where nanoparticles were once attached (Fig. 2c). When RBCs were structurally fixed *after* shear-

induced particle detachment, no indentations were seen (Fig 2d). The presence of reversible indentations suggests that adhesion of nanoparticles on RBCs is mediated by spreading of RBC membrane on the surface of hydrophobic nanoparticles. This spreading should increase the RBC-particle contact area, thus leading to a strong adhesion. However, upon shear-induced detachment, RBC's fluid membrane is able to reversibly return to its original shape.

Effect of NP on circulation of carrier RBCs

RBCs are the longest circulating cells in the body, circulating up to 120 days in humans. The effect of NP attachment on RBC circulation of RBCs was studied at two doses (low, 10:1 and high, 100:1). Attachment of NPs to RBCs at low doses did not significantly (p > 0.05) decrease circulation time of these modified RBCs compared to native RBCs at low dose (Fig. 3, open vs. hatched bars). The half-lives of RBCs with and without NPs were comparable (33.5 +/- 2.1 and 33.6 /- 5.8 hours, respectively). Attachment of NPs at higher doses (100:1) (Fig. 3, black bars) however, induced a decrease in circulation of RBCs likely due to accelerated removal of RBCs carrying multiple particles.

Biodistribution of Red Blood Cells

Next, we tested whether NP carriage affects RBC uptake in the organs. RBCs were labeled with ⁵¹Cr and their biodistribution was examined for high loaded RBCs (100:1:NP:RBC incubation). For these experiments, organs were not perfused so as to reveal the potential effect that nanoparticles may have on irreversible uptake and reversible retention of RBCs in the lumen (*i.e.*, hyperemia) in organs. At 1 hour (Fig. 4a) biodistribution of RBCs with or without NPs was comparable. Similarly, at 24 hours, organ retention of RBCs with and without NPs was near the same (Fig. 4b). Results in Fig. 4 indicate that attachment of NPs to RBCs does not influence organ distribution or retention of RBCs in spleen, which is known to sequester and clear damaged or irregular RBCs. Some differences were noted in both kidney and liver; however retention of RBCs in these organs was extremely low and does not significantly contribute to RBC clearance, compared to other organs, in either group.

Biodistribution of Nanoparticles

Carriage by RBCs cardinally changed organ distribution of nanoparticles. First, blood level of RBC–NP was ~2–3 times higher than that of free NPs (SI Fig. 2a) at all time points. Therefore, as expected, RBC carrier markedly prolongs NP circulation. Major difference in blood level between free and RBC-bound NP should be taken into account in assessing their uptake in the organs, *e.g.*, to detect nanoparticles that are retained in the tissue *vs.* those in the residual blood pool. For this, prior to assessing particle accumulation, organs were perfused to remove blood. After one hour, nanoparticle uptake in the spleen was reduced by over 50% compared to free particles (Fig. 5a, **white bars:** free nanoparticles, **black bars:** RBC-adsorbed nanoparticles). More importantly, accumulation in lungs was increased ~5-fold. Even after 24 hours, nanoparticle persistence in the lungs was still elevated (~3-fold) for RBC-adsorbed nanoparticles compared to free nanoparticles (Fig. 5b, **white bars:** free nanoparticles, **black bars:** RBC-adsorbed nanoparticles). Enhanced accumulation was also seen in brain, kidneys, intestine, skin, heart and blood at 1 hour (SI Fig. 2b, **white bars:** free nanoparticles, **black bars:** RBC-adsorbed nanoparticles).

Kinetics of Pulmonary Accumulation of RBC-carried NP

We studied the kinetics of NP biodistribution after administration in the free or RBC-adsorbed form. Free nanoparticles exhibited relatively low accumulation in lungs of about 4% ID/gram (Fig. 6a, **circles**, see SI Fig. 2c for complete NP biodistribution). The majority of the particles were deposited in the liver and spleen. In contrast, RBC-adsorbed nanoparticles exhibited high lung accumulation within 30 minutes (Fig. 6a, **squares**, see SI Fig. 2d for complete RBC+NP biodistribution). The lung accumulation of adsorbed particles was about 5-fold higher compared to that of free particles over a range of 10 hours with a maximum enhancement of 7-fold seen at 10 hours. Lung accumulation decreased and approached that of free nanoparticles after 24 hours (Fig. 6a). However, even at 24 hours, lung accumulation was significantly higher (p< 0.05) for RBC+NP groups compared to free NPs at all time points. In addition to increasing lung accumulation, RBC-adhesion also decreased liver and spleen clearance of nanoparticles.

Collectively, RBC-adhesion led to increased lung/liver accumulation ratio of nanoparticles (Fig. 6b, circles *vs.* squares) and an increased lung/spleen accumulation ratio of nanoparticles (Fig. 6c: circles *vs.* squares). Lung/liver and lung/spleen accumulation values of free nanoparticles did not change significantly over a period of 24 hours, averaging at about 0.10 for lung/liver and 0.20 for lung/spleen. In contrast, the lung/liver accumulation ratio for RBC-adhered nanoparticles changed significantly over 24 hours, peaking at a value of ~2 at 10 hours, a value over 15-fold higher than that for free nanoparticles. All lung/liver and lung/spleen ratios were significantly higher (p< 0.05) for RBC+NP groups compared to free NPs at all time points, illustrating the ability of hitchhiked nanoparticles to target lungs while avoiding reticuloendothelial system (RES) organs. Hitchhiking on RBCs also increased accumulation in kidneys and the heart, although the enhancement due to hitchhiking was less prominent than that in lungs. Interestingly, the drop in concentration seen in case of lungs at 24 hours was not seen for kidneys or heart (SI Fig. 2d).

Addition of anti-ICAM-1 Antibody

We assessed whether the drop in NP lung accumulation over 24 hours (Fig. 6a) can be mitigated by adsorption of anti-ICAM-1 antibody (Ab) on the exposed surface of NPs. NPs were first adsorbed to RBCs and anti-ICAM-1 Ab was then passively adsorbed onto the exposed carboxylated surface of NP (21.99 +/- 5.15 µg of ICAM-1 Ab per mg of particle). Confocal microscopy confirmed that anti-ICAM-1 Ab attached only to the NP surface and not to RBC membranes (Fig.7a). Biodistribution was assessed at two points, 6 hours and 24 hours as representative short and long times. Anti-ICAM-1 Ab-coated RBC+NP complexes exhibited increased lung accumulation, compared to RBC+NP with no anti-ICAM-1 Ab (Fig. 7b). Lung accumulation of NPs for RBC-NP, which otherwise decreased from 6 to 24 hours was maintained at a high level by the presence of anti-ICAM-1 Ab. Further, addition of anti-ICAM-1 further decreased liver accumulation of NPs (Fig. 7c). However, anti-ICAM-1 conjugation increased spleen retention for RBC+NP complexes at 6 hours (Fig. 7d), which is expected due to expression of anti-ICAM-1 receptor in spleen tissue. 32 Complete biodistribution for anti-ICAM-1 modified RBC+NP complexes was also determined (SI Fig. 3a and 3b).

Discussion

The results presented here demonstrate the ability of cellular hitchhiking to reduce MPS clearance and enhance accumulation in lungs. Nanoparticles were reversibly and noncovalently adsorbed on the surface of RBCs. Upon intravenous administration, particles desorbed likely due to shear (Fig. 2b) or direct RBC-endothelium contact during their passage through the tissue microvasculature. This desorption occurred rapidly as ~6% of NPs attached to RBCs remained in circulation after 30 minutes. This is well below the halflife of RBCs themselves (~33 hours). In other words, particles detach from RBCs much faster than the rate at which RBCs themselves are removed from circulation. The precise rate of NP detachment and its mechanisms require further assessment. The rate of detachment is likely to depend on the size and geometry of vasculature as well as the location of NP attachment to RBC. It is likely that NPs attached to the outer part of RBC may detach more rapidly than those attached to the central dimple. NP and RBC biodistribution data from Figs 3 and 4 together indicate that there is a transfer of nanoparticles from RBCs to endothelium in the vasculature. Transient accumulation of detached NPs in lungs (Fig. 6a) suggests that NPs that are not bound to endothelium or internalized are likely washed away by the blood over 24 hours. This is also evident from the effect of anti-ICAM-1 Ab on the retention of NPs in the vasculature. The presence of anti-ICAM-1 Ab is likely to increase binding strength of NPs to the endothelium³³ as well as lead to increased internalization, both of which will increase the persistence of NPs in endothelium. A schematic (Fig. 8) provides a hypothesis how NPs detach from RBCs in microcirculation. Based on the large amount of NPs present in lungs when adsorbed onto RBCs, their detachment from RBCs is attributed to the squeezing of RBC through tiny capillaries smaller in diameter than the RBC itself, that are present in air-blood-barrier microcirculation.³⁴ Pulmonary vasculature contains ~25–30% of total endothelial surface in the body and receives the entire venous cardiac output for oxygenation via pulmonary arterial trunk, in addition to a fraction of arterial cardiac output via intercostal and pleural vessels.³⁵ This high percentage of endothelium that receives >50% of total cardiac blood output combined with forced RBC-endothelial contact in the lung vasculature is proposed to facilitate detachment of NPs from RBCs and subsequent accumulation in lungs. Uptake in lung is unlikely to be mediated by macrophages. While some mammalian species have macrophages active in endothelium, this is typically not the case for healthy rodents. 36–38 Further, the lung macrophages are present on the air side of the vasculature; hence the NPs will make first contact with endothelial cells and not macrophages.

RBC-hitchhiking thus provides a natural means to deliver nanoparticles in the close vicinity of vascular endothelium in lungs. The beneficial effects of RBC-adhesion mediated NP delivery are expected to be higher in tissues with extensive microvascular networks as is the case for lungs. Mouse lung capillaries possess an average diameter of 5 μ m reaching sizes as small as 1 μ m, 3–4 times smaller than RBC diameters to enable their close contact with the endothelium so as to facilitate oxygen transport. The close contact likely plays a role in dislodging of nanoparticles.

RBC-bound NPs circulate for much longer and in higher percentages than freely administered NPs. Circulation and organ distribution of RBCs themselves was not impaired

due to NP attachment. To ensure that ³H-NP signal was due to NPs and not blood remaining in organs, organs were perfused for all NP-tracing experiments. This ensures that the measured NP biodistribution corresponds to NPs that have either detached from RBCs and bound to endothelium or have been internalized by the endothelium. On the other hand, for ⁵¹Cr-RBC tracing experiments, organs were not perfused so as to examine the effect NP attachment had on RBC biodistribution. Circulation and biodistribution of independently traced RBC-bound ³H-labeled-NPs and ⁵¹Cr-labeled-RBCs indicate a true transfer of NPs from RBCs to endothelium. Dislodged nanoparticles remain in tissues either due to nonspecific interactions with the endothelium or due to internalization by the cells. Persistence of nanoparticle accumulation in tissues was found to depend on the tissue type and was extended, in case of lungs, by conjugation of anti-ICAM-1 Ab to NP surface for RBC/NP complexes. For RBC/NP complexes, enhanced accumulation persisted in heart and kidneys for a period of 24 hours, the accumulation peaked at 10 hours for lungs followed by a substantial decline by 24 hours. However, after conjugation with anti-ICAM-1, %ID/gram in lungs and persistence in lungs at 24 hours was significantly increased (Fig. 7b). Nanoparticles were able to avoid the liver and spleen over a period of 24 hours when attached to RBCs. Liver and spleen are known to rapidly remove all foreign entities from blood and developing nanoparticle therapies which both target other organs while avoiding liver and spleen has been a challenge.³⁹

Adhesion of nanoparticles did not produce adverse effects on RBCs. No significant impact of nanoparticle adhesion on the morphology or function of RBCs was seen. No hemolysis of RBCs due to nanoparticle adhesion was observed. The only change seen in the membrane morphology was directly underneath the membrane, which appeared to be induced by spreading of the RBC membrane on the particle surface. However, this change was reversible. Physically damaged cells are generally removed from the circulation predominately by the spleen⁴⁰ and to a less extent by the liver;⁴¹ therefore it is imperative that RBC morphology not be significantly altered as RBCs must perform their natural functions when nanoparticles are attached. Further, since no statistical difference in RBC accumulation for either unmodified RBCs or NP loaded RBCs was noted in spleen at any time point, it is not expected that NP modification of RBCs is affecting clearance in this major RBC clearance organ. Previous studies have shown that while nanoparticles are ultimately removed from the circulation, RBCs which once carried nanoparticles continue to remain in circulation.²³ Further, the fraction of total RBCs in circulation that were labeled by nanoparticles in these experiments was small (1.7%). Hence, the likelihood of nanoparticles-laden RBCs significantly impacting overall circulation is negligible.

Simultaneously, NP conjugation to RBCs enhances the accumulation of NPs in highly vascularized organs, first of as all, lungs. Due to extended surface area and privileged perfusion by >50% of the total cardiac blood output, pulmonary endothelium represents a preferential target, 42 in particular, for antibodies to endothelial surface determinants including anti-ICAM-1.43, 44 In this vein, by conjugating anti-ICAM-1 to RBC/NP complexes, persistence of NPs targeted to lung can be maintained over a period of 24 hours while RBC/NP lung persistence, without anti-ICAM-1 modification, is limited to much shorter times.

At a fundamental level, the use of RBC-adsorbed NPs provides a new hybrid approach for drug delivery. Synthetic systems such as polymeric nanoparticles offer the advantages of control over particle composition and manufacturability; however, they suffer from the limitation of immune clearance. RBCs, on the other hand, naturally avoid RES clearance for four months and continuously reach all tissues. An approach based on the use of synthetic nanoparticles to encapsulate drugs and deliver them to tissues using RBCs offers an optimal blend of natural and synthetic systems. RBC-adsorption also provides an ideal blend of enhanced circulation and targeting. Currents means of enhancing circulation are based on the use of PEG or polaxamers, which suffer from limited circulation times and accelerated clearance after repeat injections. $^{21, 45, 46}$ The ability of RBC-hitchhiking NPs to exhibit longer circulation and tissue deposition after repeat injections needs further investigations. Several additional questions need to be answered before full potential of RBC-mediated NP delivery can be realized. These include understanding the fate of NPs in organs, limits of NP loading on RBCs and behavior of NPs after repeat injections. It should also be noted that this method requires the use of a patient's own blood cells or the use of any other RBCs that can be transfused into patients.

Hitchhiking onto mammalian cells is also observed in nature by certain pathogens such as *Mycoplasma haemofelis* (previously known as haemobartonella), which remain circulating inside mammals by hitchhiking on the surface of RBCs.⁴⁷ Recently, hitchhiking onto the surface of mammalian cells has received attention as a new approach of drug delivery. Specifically, RBCs have been used to prolong *in vivo* circulation of nanoparticles.^{23, 24} The results reported here build on these findings and demonstrate tissue accumulation of nanoparticles. In addition, T cells have also been used for cellular hitchhiking, where drug loaded liposomes were conjugated directly to T cell surface for efficient elimination of EG7-OVA and EL4 tumors.⁴⁸ Additional systems are also being developed based on specific cell surface receptors present on B cells, monocytes, and macrophages for attachment of drug carrying backpacks.^{49, 50}

Cellular-hitchhiking provides a novel means to address two major issues that nanoparticle therapies routinely face; the avoidance of MPS organs, liver and spleen and targeted delivery to difficult-to-reach sites in body such as brain and lungs. While studies reported here were performed with non-biodegradable polystyrene particles, RBC hitchhiking can be extended to biodegradable PLGA nanoparticles (SI Fig. 4). With further research focused on understanding the mechanisms of particle detachment from RBCs and their interactions with the endothelium, RBC-hitchhiking nanoparticles may open new opportunities on therapeutic delivery.

Methods

Blood Collection and storage

Whole blood was collected from healthy female BALB/c mice (18–20g; 8–10 weeks old). Mice were sacrificed by CO₂ overdose and blood was collected *via* cardiac puncture and stored in heparin coated tubes. Blood was stored at 4°C for no longer than 2 days for all experiments. Blood was re-suspended in 4% sodium citrate (pH 7.4). Whole blood was

centrifuged at room temperature at 100g and supernatant was discarded leaving purified red blood cells.

Particle Preparation

Fluorescently and non-fluorescently labeled Carboxylated polystyrene (PS) particles (200 nm) were purchased from Polysciences. Particles were radiolabeled with tritium (³H) conjugated oleic acid (Moravek Biochemicals). Briefly, 20% w/v PS particles in water were added to a solution containing 100µl ³H-oleic acid, 100µl ethanol, and 25µl tetrahydrofuran for 30 minutes with constant rotation. Particles were then washed ten times *via* centrifugation for 30 minutes at 15000g to remove unincorporated oleic acid.

PLGA nanoparticles were prepared *via* standard nano-precipitation techniques. Briefly, an organic phase with 75mg PLGA polymer in 7.5ml acetone opposite an aqueous 2% poly vinyl alcohol solution. The organic phase was added drop wise to the aqueous phase using a syringe pump at 15ml/hr with continuous stirring (300rpm). PLGA nanoparticles were purified *via* centrifugation and characterized using TEM.

Attachment of Nanoparticles to RBCs

Nanoparticles and RBCs were suspended in 4% sodium citrate. A known number of nanoparticles were incubated with RBCs at room temperature for 30 minutes. Unbound nanoparticles were separated from RBCs with bound nanoparticles *via* centrifugation. anti-ICAM-1 Ab was added to RBC-nanoparticle conjugates at a concentration of 400 µg/ml in PBS for 1 hour under constant rotation. Detachment of particles performed under shear was performed using an AR-G2 rheometer from TA Instruments. Particle-RBC conjugates were re-suspended in plasma proteins and serum prior to detachment in order to prevent reattachment of nanoparticles. Particle-RBC conjugates were exposed to 5 Pa of shear stress for 15 minutes at 37°C. Detachment was visually confirmed using a scanning electron microscope (see below).

Fluorescence-activated cell sorting (FACS)

Nanoparticles, red blood cells and conjugates were suspended in PBS. A FACSAria Flow Cytometer with a 70um nozzle was used to quantify attachment of nanoparticles to red blood cells. Mammalian cells were filtered prior to analyzing sample. BD FACSDiva software 6.0 was used to analyze data.

Scanning electron microscopy (SEM)

An FEI XL40 SEM at 3–5kV with a 5mm working distance was used for imaging both cells and particles. Images were taken after 2 minutes of palladium coating (at 10kV) *via* a Hummer sputtering system. Cells were imaged in a dehydrated state and prepared using standard cell surface fixation technique. Briefly, cell samples were incubated with a 2.5% glutaraldehyde solution for the cross-linking of surface proteins. This provides cells with the required stability live tissue samples do not possess which is necessary while imaging under high voltage and vacuum.

Transmission electron microscopy (TEM)

An FEI T20 was used to characterize PLGA nanoparticles. 2µl of diluted PLGA nanoparticles were deposited on a copper grid and dried in air prior to imaging.

Confocal microscopy

An Olympus Fluoview 500 (Olympus America Inc. Center Valley, PA, USA) was used to image fluorescently labeled anti-ICAM-1 Ab modified NPs attached to RBCs.

Tissue distribution and blood clearance of RBC/NPs in mice

⁵¹Cr-labeled mouse RBCs (⁵¹Cr-RBC) were prepared as described⁵¹ and ⁵¹Cr-RBC/NP groups were prepared as discussed earlier. Naive BALB/c female mice (18–20 g; n= 3–6 per group) were anesthetized and injected intravenously *via* jugular vein with approximately 10uCi of ⁵¹Cr-RBC or ⁵¹Cr-RBC/NP formulations. At designated time points post-injection, blood was collected from the retro-orbital sinus and organs (kidneys, liver, spleen, and lung) were collected and weighed. Blood samples were withdrawn in heparin tubes, centrifuged at 1200*g*, and radioactivity in plasma, RBC pellets, and organs was measured in a gamma-counter.

In vivo Biodistribution

For nanoparticle biodistribution studies, 5×10^9 radiolabeled particles in Alsever's buffer were injected *via* tail vein into healthy female BALB/c mice (18–20g; n=3–5 per group). At predetermined time points, mice were anesthetized and euthanized by opening of the chest cavity and perfusion of PBS through the left ventricle. Known weights of liver, spleen, kidney, heart, lungs, brain, intestine, skin, and blood were harvested and dissolved overnight in Solvable (Perkin Elmer). The following morning, liquid scintillation counting efficiency cocktail Ultima Gold (Perkin Elmer) was added to organ solutions and organs were measured for their radioactive content in a Packard TriCarb 2100TR scintillation counter. All animal protocols were approved by respective Institutional Animal Care and Use Committees (IACUC) at the University of California, Santa Barbara.

Supplementary Material

Refer to Web version on PubMed Central for supplementary material.

Acknowledgments

A.C.A. was supported by the National Science Foundation Graduate Research Fellowship under Grant No. DGE-1144085.The MRL Central Facilities are supported by the MRSEC Program of the NSF under Award No. DMR 1121053; a member of the NSF-funded Materials Research Facilities Network (www.mrfn.org). This study was supported in part by NIH *via* grants to VRM (HL087036, HL090697 and HL121134). Authors would like to thank P. Cheng and M. Helgeson of UCSB for rheometer use and training.

References

- Azarmi S, Roa WH, Lobenberg R. Targeted Delivery of Nanoparticles for the Treatment of Lung Diseases. Adv. Drug Delivery Rev. 2008; 60:863–875.
- 2. Faraji AH, Wipf P. Nanoparticles in Cellular Drug Delivery. Bioorg. Med. Chem. 2009; 17:2950–2962. [PubMed: 19299149]

3. Wang AZ, Langer R, Farokhzad OC. Nanoparticle Delivery of Cancer Drugs. Annu. Rev. Med. 2012; 63:185–198. [PubMed: 21888516]

- 4. Dhar S, Gu FX, Langer R, Farokhzad OC, Lippard SJ. Targeted Delivery of Cisplatin to Prostate Cancer Cells by Aptamer Functionalized Pt(Iv) Prodrug-Plga-Peg Nanoparticles. Proc. Natl. Acad. Sci. U. S. A. 2008; 105:17356–17361. [PubMed: 18978032]
- 5. Peer D, Karp JM, Hong S, Farokhzad OC, Margalit R, Langer R. Nanocarriers as an Emerging Platform for Cancer Therapy. Nat. Nanotechnol. 2007; 2:751–760. [PubMed: 18654426]
- Brannon-Peppas L, Blanchette JO. Nanoparticle and Targeted Systems for Cancer Therapy. Adv. Drug Deliv. Rev. 2004; 56:1649–1659. [PubMed: 15350294]
- Davis ME, Chen ZG, Shin DM. Nanoparticle Therapeutics: An Emerging Treatment Modality for Cancer. Nat. Rev. Drug Discovery. 2008; 7:771–782.
- 8. Hrkach J, Von Hoff D, Mukkaram Ali M, Andrianova E, Auer J, Campbell T, De Witt D, Figa M, Figueiredo M, Horhota A, et al. Preclinical Development and Clinical Translation of a Psma-Targeted Docetaxel Nanoparticle with a Differentiated Pharmacological Profile. Sci. Transl. Med. 2012; 4:128ra39.
- 9. Kattan J, Droz JP, Couvreur P, Marino JP, Boutan-Laroze A, Rougier P, Brault P, Vranckx H, Grognet JM, Morge X, et al. Phase I Clinical Trial and Pharmacokinetic Evaluation of Doxorubicin Carried by Polyisohexylcyanoacrylate Nanoparticles. Invest. New Drugs. 1992; 10:191–199. [PubMed: 1428729]
- Green MR, Manikhas GM, Orlov S, Afanasyev B, Makhson AM, Bhar P, Hawkins MJ. Abraxane, a Novel Cremophor-Free, Albumin-Bound Particle Form of Paclitaxel for the Treatment of Advanced Non-Small-Cell Lung Cancer. Ann. Oncol. 2006; 17:1263–1268. [PubMed: 16740598]
- 11. Hofheinz RD, Gnad-Vogt SU, Beyer U, Hochhaus A. Liposomal Encapsulated Anti-Cancer Drugs. Anticancer Drugs. 2005; 16:691–707. [PubMed: 16027517]
- Allen TM, Cullis PR. Drug Delivery Systems: Entering the Mainstream. Science. 2004; 303:1818– 1822. [PubMed: 15031496]
- 13. Ruoslahti E. Peptides as Targeting Elements and Tissue Penetration Devices for Nanoparticles. Adv. Mater. 2012; 24:3747–3756. [PubMed: 22550056]
- Yoo JW, Chambers E, Mitragotri S. Factors That Control the Circulation Time of Nanoparticles in Blood: Challenges, Solutions and Future Prospects. Curr. Pharm. Des. 2010; 16:2298–2307. [PubMed: 20618151]
- 15. Riehemann K, Schneider SW, Luger TA, Godin B, Ferrari M, Fuchs H. Nanomedicine--Challenge and Perspectives. Angew. Chem., Int. Ed. Engl. 2009; 48:872–897. [PubMed: 19142939]
- 16. Sanhai WR, Sakamoto JH, Canady R, Ferrari M. Seven Challenges for Nanomedicine. Nat. Nanotechnol. 2008; 3:242–244. [PubMed: 18654511]
- 17. Perry JL, Reuter KG, Kai MP, Herlihy KP, Jones SW, Luft JC, Napier M, Bear JE, DeSimone JM. Pegylated Print Nanoparticles: The Impact of Peg Density on Protein Binding, Macrophage Association, Biodistribution, and Pharmacokinetics. Nano Lett. 2012; 12:5304–5310. [PubMed: 22920324]
- Bazile D, Prud'homme C, Bassoullet MT, Marlard M, Spenlehauer G, Veillard M. Stealth Me.Peg-Pla Nanoparticles Avoid Uptake by the Mononuclear Phagocytes System. J. Pharm. Sci. 1995; 84:493–498. [PubMed: 7629743]
- 19. Ishida T, Maeda R, Ichihara M, Irimura K, Kiwada H. Accelerated Clearance of Pegylated Liposomes in Rats after Repeated Injections. J. Controlled Release. 2003; 88:35–42.
- Ishida T, Masuda K, Ichikawa T, Ichihara M, Irimura K, Kiwada H. Accelerated Clearance of a Second Injection of Pegylated Liposomes in Mice. Int. J. Pharm. 2003; 255:167–174. [PubMed: 12672612]
- 21. Ishida T, Ichihara M, Wang X, Yamamoto K, Kimura J, Majima E, Kiwada H. Injection of Pegylated Liposomes in Rats Elicits Peg-Specific Igm, Which Is Responsible for Rapid Elimination of a Second Dose of Pegylated Liposomes. J. Controlled Release. 2006; 112:15–25.
- 22. Rodriguez PL, Harada T, Christian DA, Pantano DA, Tsai RK, Discher DE. Minimal "Self" Peptides That Inhibit Phagocytic Clearance and Enhance Delivery of Nanoparticles. Science. 2013; 339:971–975. [PubMed: 23430657]

 Chambers E, Mitragotri S. Prolonged Circulation of Large Polymeric Nanoparticles by Non-Covalent Adsorption on Erythrocytes. J. Controlled Release. 2004; 100:111–119.

- Chambers E, Mitragotri S. Long Circulating Nanoparticles Via Adhesion on Red Blood Cells:
 Mechanism and Extended Circulation. Exp. Biol. Med. (Maywood, NJ, U.S.). 2007; 232:958–966.
- Muzykantov VR, Sakharov DV, Smirnov MD, Domogatsky SP, Samokhin GP. Targeting of Enzyme Immobilized on Erythrocyte Membrane to Collagen-Coated Surface. FEBS Lett. 1985; 182:62–66. [PubMed: 3972125]
- 26. Muzykantov VR. Drug Delivery by Red Blood Cells: Vascular Carriers Designed by Mother Nature. Exper. Opin. Drug Delivery. 2010; 7:403–427.
- 27. Muzykantov VR, Sakharov DV, Smirnov MD, Samokhin GP, Smirnov VN. Immunotargeting of Erythrocyte-Bound Streptokinase Provides Local Lysis of a Fibrin Clot. Biochim. et Biophys. Acta. 1986; 884:355–362.
- 28. Zaitsev S, Spitzer D, Murciano JC, Ding BS, Tliba S, Kowalska MA, Marcos-Contreras OA, Kuo A, Stepanova V, Atkinson JP, et al. Sustained Thromboprophylaxis Mediated by an Rbc-Targeted Pro-Urokinase Zymogen Activated at the Site of Clot Formation. Blood. 2010; 115:5241–5248. [PubMed: 20410503]
- Danielyan K, Ganguly K, Ding BS, Atochin D, Zaitsev S, Murciano JC, Huang PL, Kasner SE, Cines DB, Muzykantov VR. Cerebrovascular Thromboprophylaxis in Mice by Erythrocyte-Coupled Tissue-Type Plasminogen Activator. Circulation. 2008; 118:1442–1449. [PubMed: 18794394]
- 30. Yoon J-Y, Kim J-H, Kim W-S. Interpretation of Protein Adsorption Phenomena onto Functional Microspheres. Colloids Surf., B. 1998; 12:15–22.
- Yoon J-Y, Park H-Y, Kim J-H, Kim W-S. Adsorption of Bsa on Highly Carboxylated Microspheres—Quantitative Effects of Surface Functional Groups and Interaction Forces. J. Colloid and Interface Sci. 1996; 177:613–620.
- 32. Hayes SH, Seigel GM. Immunoreactivity of Icam-1 in Human Tumors, Metastases and Normal Tissues. Int. J. Clin. Exp. Pathol. 2009; 2:553. [PubMed: 19636402]
- 33. Kolhar P, Anselmo AC, Gupta V, Pant K, Prabhakarpandian B, Ruoslahti E, Mitragotri S. Using Shape Effects to Target Antibody-Coated Nanoparticles to Lung and Brain Endothelium. Proc. Natl. Acad. Sci. U. S. A. 2013; 110:10753–10758. [PubMed: 23754411]
- Sikora L, Johansson AC, Rao SP, Hughes GK, Broide DH, Sriramarao P. A Murine Model to Study Leukocyte Rolling and Intravascular Trafficking in Lung Microvessels. Am. J. Pathol. 2003; 162:2019–2028. [PubMed: 12759257]
- 35. Fishman A. Dynamics of the Pulmonary Circulation. Handb. Physiol. 1963; 2:1667–1743.
- Brain JD, Molina RM, DeCamp MM, Warner AE. Pulmonary Intravascular Macrophages: Their Contribution to the Mononuclear Phagocyte System in 13 Species. Am. J. Physiol.: Lung Cell. Mol. Physiol. 1999; 276:L146–L154.
- 37. Warner A, Barry B, Brain J. Pulmonary Intravascular Macrophages in Sheep: Morphology and Function of a Novel Constituent of the Mononuclear Phagocyte System. Lab. Invest. 1986; 55:276–288. [PubMed: 3747447]
- 38. Warner AE, Brain JD. Intravascular Pulmonary Macrophages: A Novel Cell Removes Particles from Blood. Am. J. Physiol. 1986; 250:R728–R732. [PubMed: 3963241]
- 39. Moghimi SM, Hunter AC, Murray JC. Long-Circulating and Target-Specific Nanoparticles: Theory to Practice. Pharmacol. Rev. 2001; 53:283–318. [PubMed: 11356986]
- 40. CROSBY WH. Normal Functions of the Spleen Relative to Red Blood Cells: A Review. Blood. 1959; 14:399–408. [PubMed: 13638340]
- 41. Terpstra V, van Berkel TJ. Scavenger Receptors on Liver Kupffer Cells Mediate the in Vivo Uptake of Oxidatively Damaged Red Blood Cells in Mice. Blood. 2000; 95:2157–2163. [PubMed: 10706889]
- 42. Muzykantov VR. Biomedical Aspects of Targeted Delivery of Drugs to Pulmonary Endothelium. Exper. Opin. Drug Delivery. 2005; 2:909–926.
- 43. Muro S, Garnacho C, Champion JA, Leferovich J, Gajewski C, Schuchman EH, Mitragotri S, Muzykantov VR. Control of Endothelial Targeting and Intracellular Delivery of Therapeutic

- Enzymes by Modulating the Size and Shape of Icam-1-Targeted Carriers. Mol. Ther. 2008; 16:1450–1458. [PubMed: 18560419]
- 44. Scherpereel A, Wiewrodt R, Christofidou-Solomidou M, Gervais R, Murciano JC, Albelda SM, Muzykantov VR. Cell-Selective Intracellular Delivery of a Foreign Enzyme to Endothelium in Vivo Using Vascular Immunotargeting. FASEB J. 2001; 15:416–426. [PubMed: 11156957]
- 45. Ishihara T, Takeda M, Sakamoto H, Kimoto A, Kobayashi C, Takasaki N, Yuki K, Tanaka K, Takenaga M, Igarashi R, et al. Accelerated Blood Clearance Phenomenon Upon Repeated Injection of Peg-Modified Pla-Nanoparticles. Pharm. Res. 2009; 26:2270–2279. [PubMed: 19633820]
- 46. Ishida T, Harada M, Wang XY, Ichihara M, Irimura K, Kiwada H. Accelerated Blood Clearance of Pegylated Liposomes Following Preceding Liposome Injection: Effects of Lipid Dose and Peg Surface-Density and Chain Length of the First-Dose Liposomes. J. Controlled Release. 2005; 105:305–317.
- 47. Criado-Fornelio A, Martinez-Marcos A, Buling-Sarana A, Barba-Carretero JC. Presence of Mycoplasma Haemofelis, Mycoplasma Haemominutum and Piroplasmids in Cats from Southern Europe: A Molecular Study. Vet. Microbiol. 2003; 93:307–317. [PubMed: 12713893]
- 48. Stephan MT, Moon JJ, Um SH, Bershteyn A, Irvine DJ. Therapeutic Cell Engineering with Surface-Conjugated Synthetic Nanoparticles. Nat Med. 2010; 16:1035–1041. [PubMed: 20711198]
- Doshi N, Swiston AJ, Gilbert JB, Alcaraz ML, Cohen RE, Rubner MF, Mitragotri S. Cell-Based Drug Delivery Devices Using Phagocytosis-Resistant Backpacks. Adv. Mater. 2011; 23:H105– H109. [PubMed: 21365691]
- Swiston AJ, Gilbert JB, Irvine DJ, Cohen RE, Rubner MF. Freely Suspended Cellular "Backpacks" Lead to Cell Aggregate Self-Assembly. Biomacromolecules. 2010; 11:1826–1832. [PubMed: 20527876]
- 51. Muzykantov VR, Seregina N, Smirnov MD. Fast Lysis by Complement and Uptake by Liver of Avidin-Carrying Biotinylated Erythrocytes. Int. J. Artif. Organs. 1992; 15:622–627. [PubMed: 1428212]

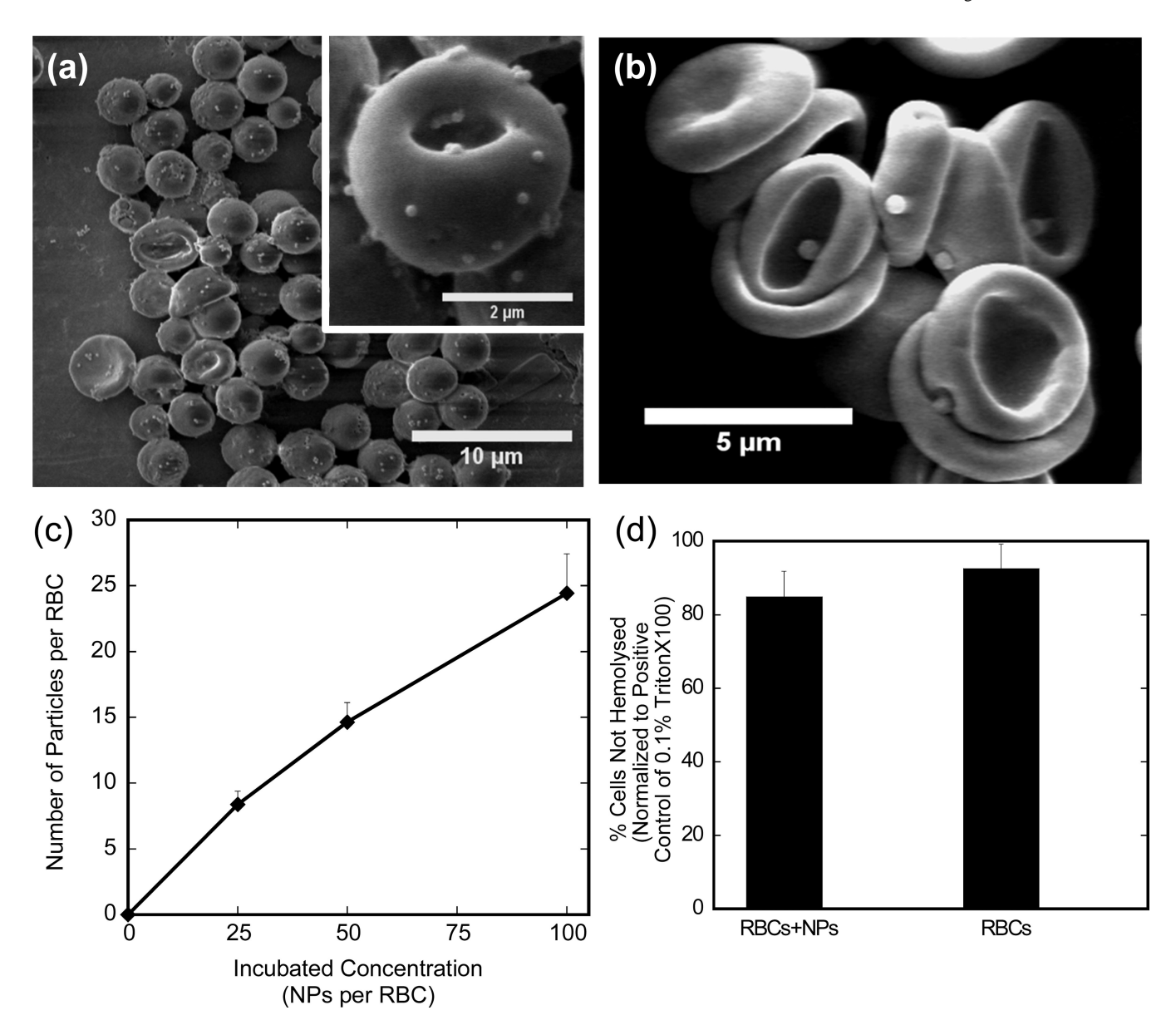


Figure 1. Attachment of nanoparticles to red blood cells
(a) Scanning electron micrographs of 200nm polystyrene spheres attached to RBCs. (b)
Scanning electron micrographs of 500nm polystyrene spheres attached to RBCs. (c)
Analysis of RBC-bound 200nm particles *via* ³H - labeling showing average number of nanoparticles attached per RBC with increasing particle concentration. Values represent mean ± SD (n=3). (d) RBCs+NPs at high loading (100:1 NP:RBC loading ratio) show no significant lysis compared to RBCs in identical buffer. Data is normalized to a positive control of 1% Triton-X-100. Values represent mean ± SD (n=3).

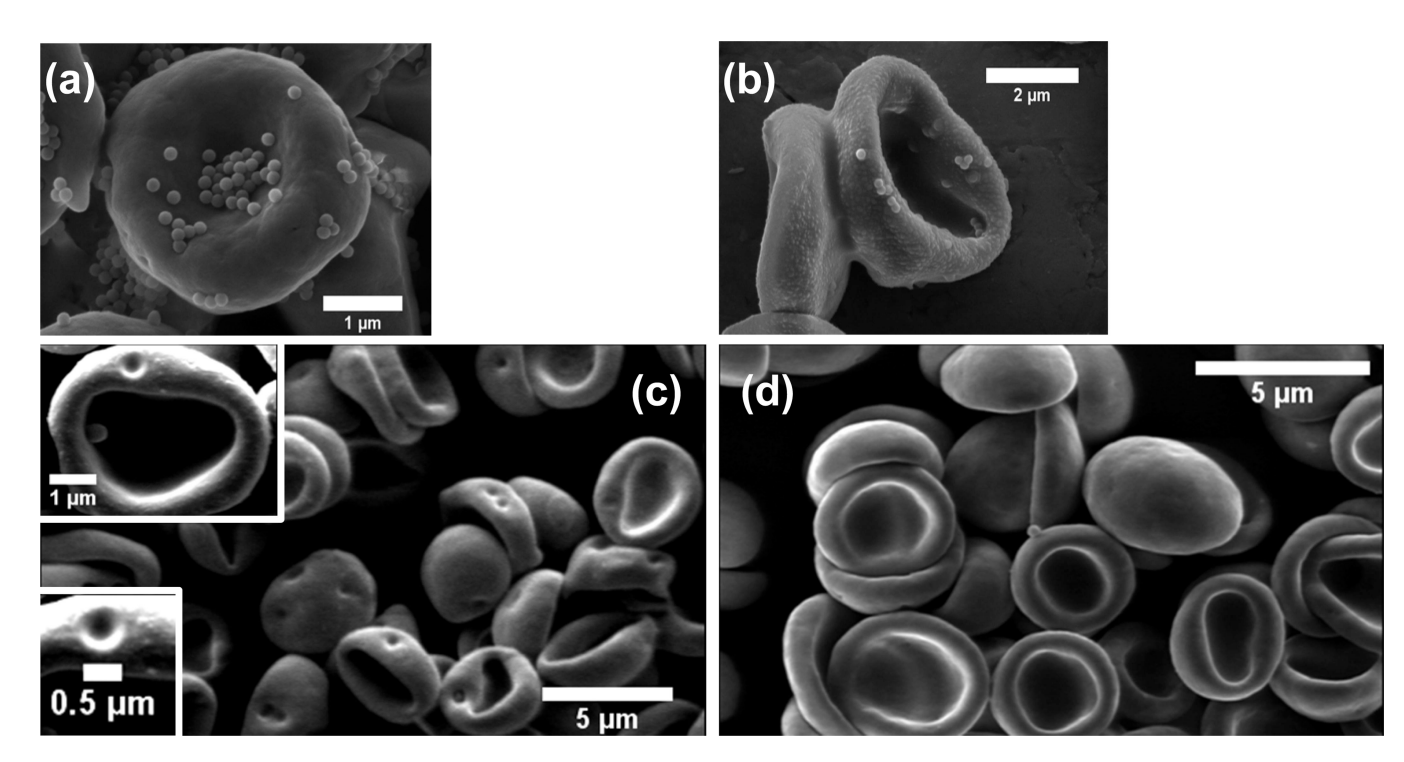


Figure 2. Detachment of nanoparticles from red blood cells

Controlled detachment of nanoparticles from RBC surface *via* applied shear stress using a rheometer: (a) no induced shear, and (b) 5 Pa shear stress for 15 minutes at 37°C. (c) Scanning electron micrographs of 500nm polystyrene spheres detached from RBCs *after* fixation with glutaraldehyde showing indents caused by particles attachment and (d) scanning electron micrographs of 500nm polystyrene spheres detached from RBCs *prior* to fixation with glutaraldehyde showing that indents are reversible and do not permanently deform RBCs.

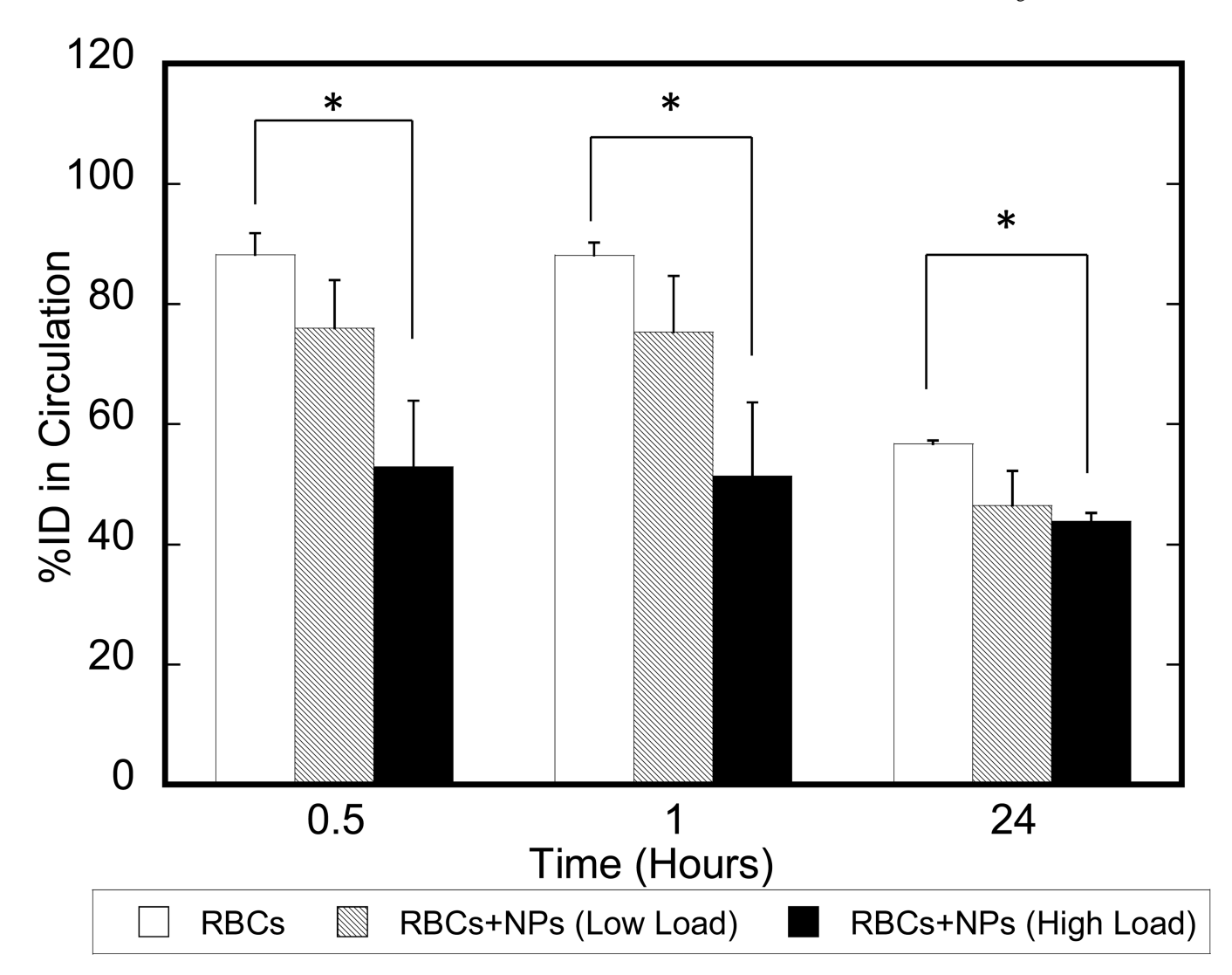


Figure 3. Time-dependent *in vivo* circulation of 51 Cr-RBCs Bar graph representing percentage of injected dose (%ID) for free 51 Cr-RBCs (white), 51 Cr-RBCs with nanoparticles attached at low loading of 1:10 (hatched), and 1:100 (black) incubation ratios (RBCs:NPs) over a 24 hour period. Values represent mean \pm SEM (n=3–6) * Denotes statistically different from labeled groups (p< 0.05).

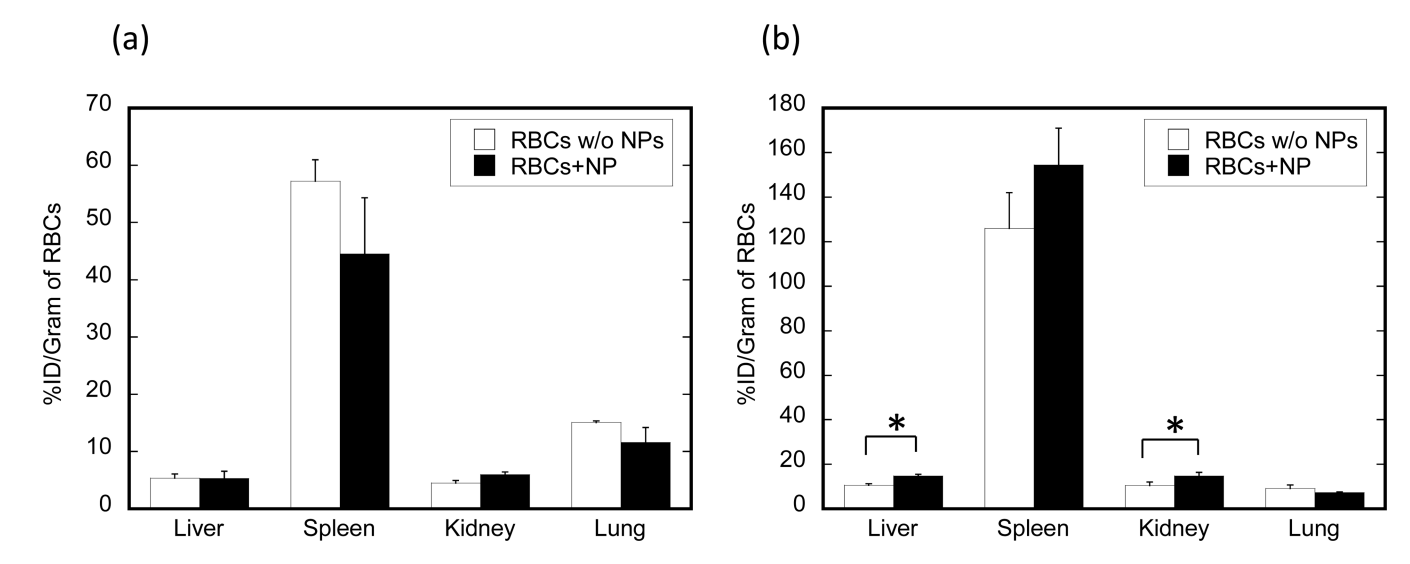
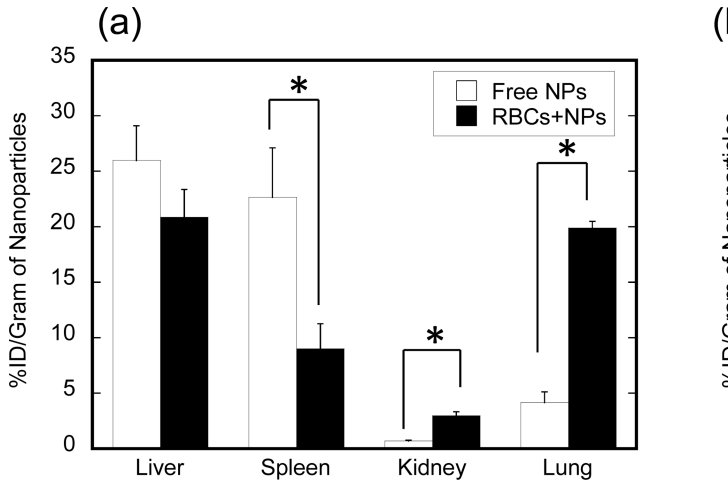


Figure 4. Time-dependent *in vivo* **biodistribution of** $^{51}\text{Cr-RBCs}$ Bar graph representing percentage of injected dose per gram of organ tissue (%ID/g) for free $^{51}\text{Cr-RBCs}$ (white), and $^{51}\text{Cr-RBCs}$ with nanoparticles attached (black) at (a) short (1 hour) and (b) long (24 hour) times. Values represent mean \pm SEM (n=3–6). * Denotes statistically different from labeled groups (p< 0.05).



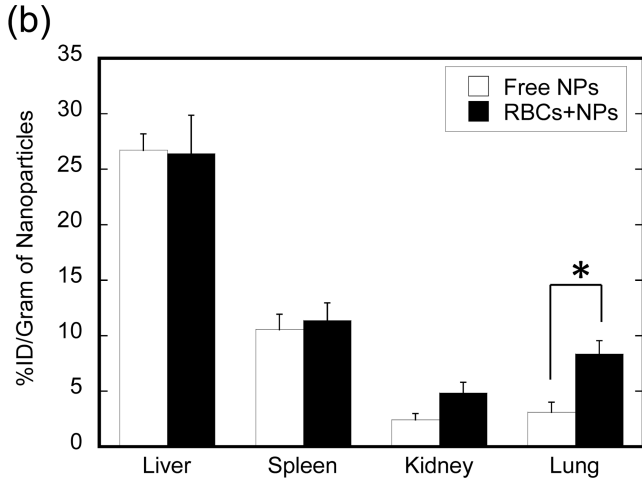


Figure 5. Time-dependent *in vivo* **biodistribution of** ³**H-nanoparticles** Bar graph representing percentage of injected dose per gram of organ tissue (% ID/g) for free ³H-nanoparticles (white), and RBC bound ³H-nanoparticles (black) at (a) short (1 hour) and (b) long (24 hour) times. Values represent mean \pm SEM (n=3–5). * Denotes statistically different from labeled groups (p< 0.05).

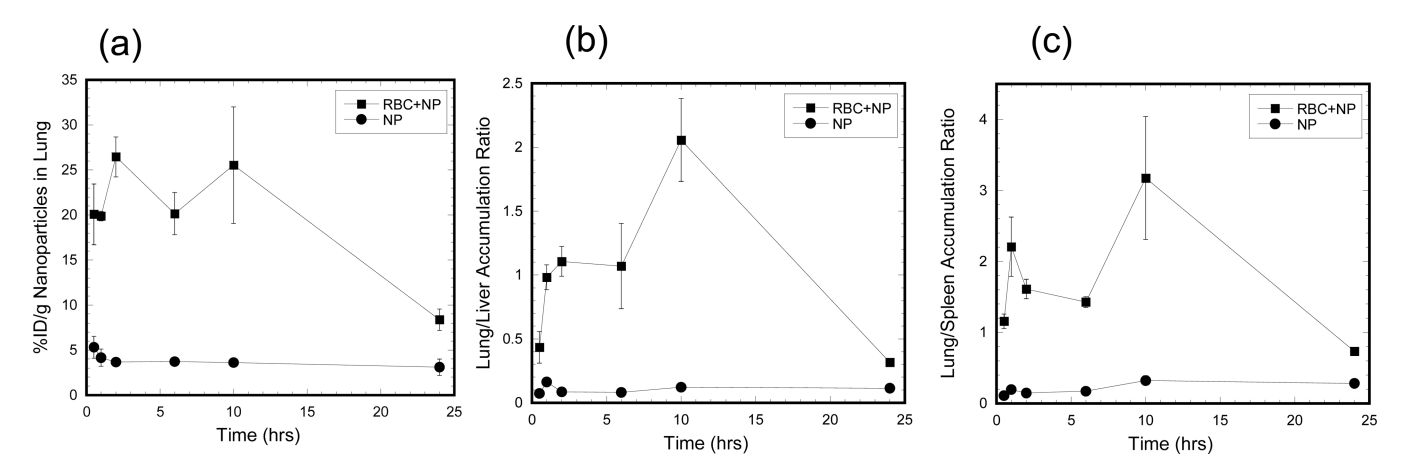
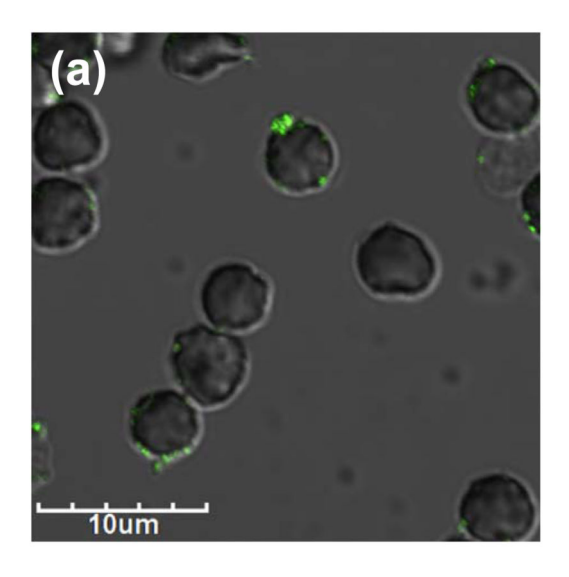
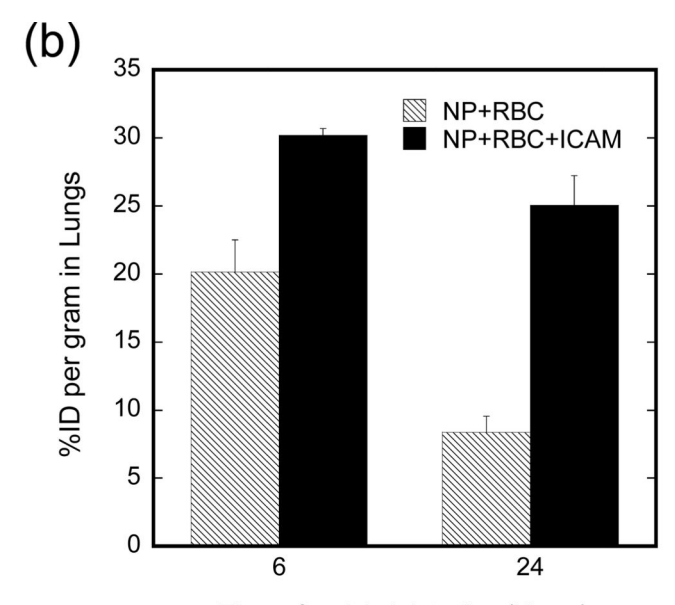
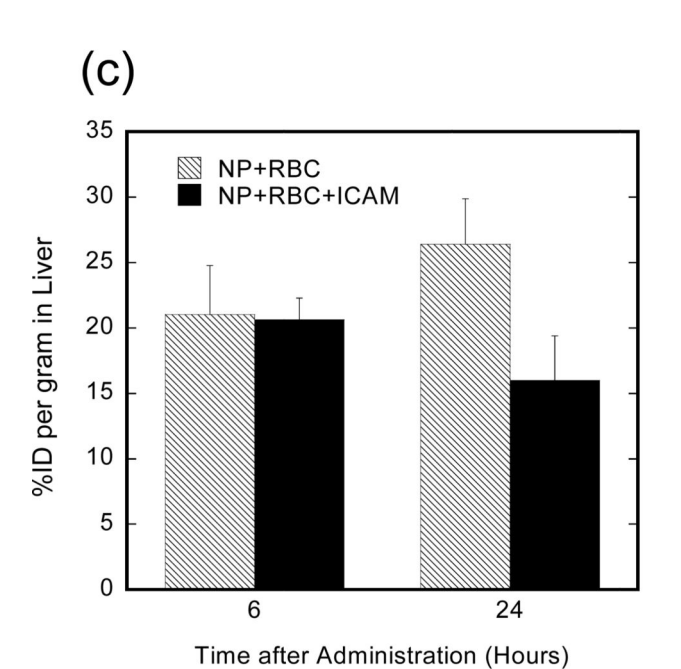


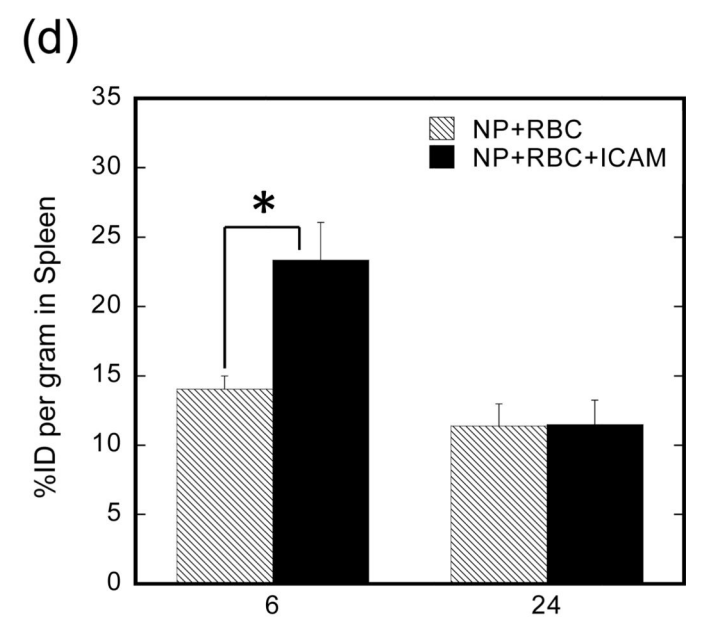
Figure 6. Kinetics of 3 H-nanoparticle targeting to lungs while avoiding clearance organs (a) 3 H-Nanoparticle accumulation in lungs represented as percentage of injected dose per gram of lung tissue (%ID/g) for free 3 H-nanoparticles (circles), and RBC bound 3 H-nanoparticles (squares). (b) Lung to liver ratio of 3 H-nanoparticle accumulation represented as percentage of injected dose per gram of organ tissue (%ID/g) for free 3 H-nanoparticles (circles), and RBC bound 3 H-nanoparticles (squares). (c) Lung to spleen ratio of 3 H-nanoparticle accumulation represented as percentage of injected dose per gram of organ tissue (%ID/g) for free 3 H-nanoparticles (circles), and RBC bound 3 H-nanoparticles (squares). Values represent mean \pm SEM (n=3–5). All RBC+NPs groups were statistically different (p< 0.05) from NP alone groups at all time points for each panel (a,b,c).





Time after Administration (Hours)





Time after Administration (Hours)

Figure 7. *In vivo* biodistribution of anti-ICAM-1-coated RBC-bound nanoparticles (a) Confocal image of fluorescently labeled anti-ICAM-1 binding only to 200nm PS spheres and not RBC membranes. (b) Lung accumulation (%ID/gram) of RBC/NP (hatched bars) and RBC/NP+anti-ICAM-1 (black bars) complexes at 6 and 24 hours. Both lung %ID/gram groups were statistically different (p < 0.05). (c) Liver accumulation (%ID/gram) of RBC –NP (hatched bars) and RBC/NP+anti-ICAM-1 (black bars) complexes at 6 and 24 hours. (d) Spleen accumulation (%ID/gram) of RBC/NP (hatched bars) and RBC–NP+anti-ICAM-1 (black bars) complexes at 6 and 24 hours. *Denotes statistically different from labeled groups (p< 0.05).

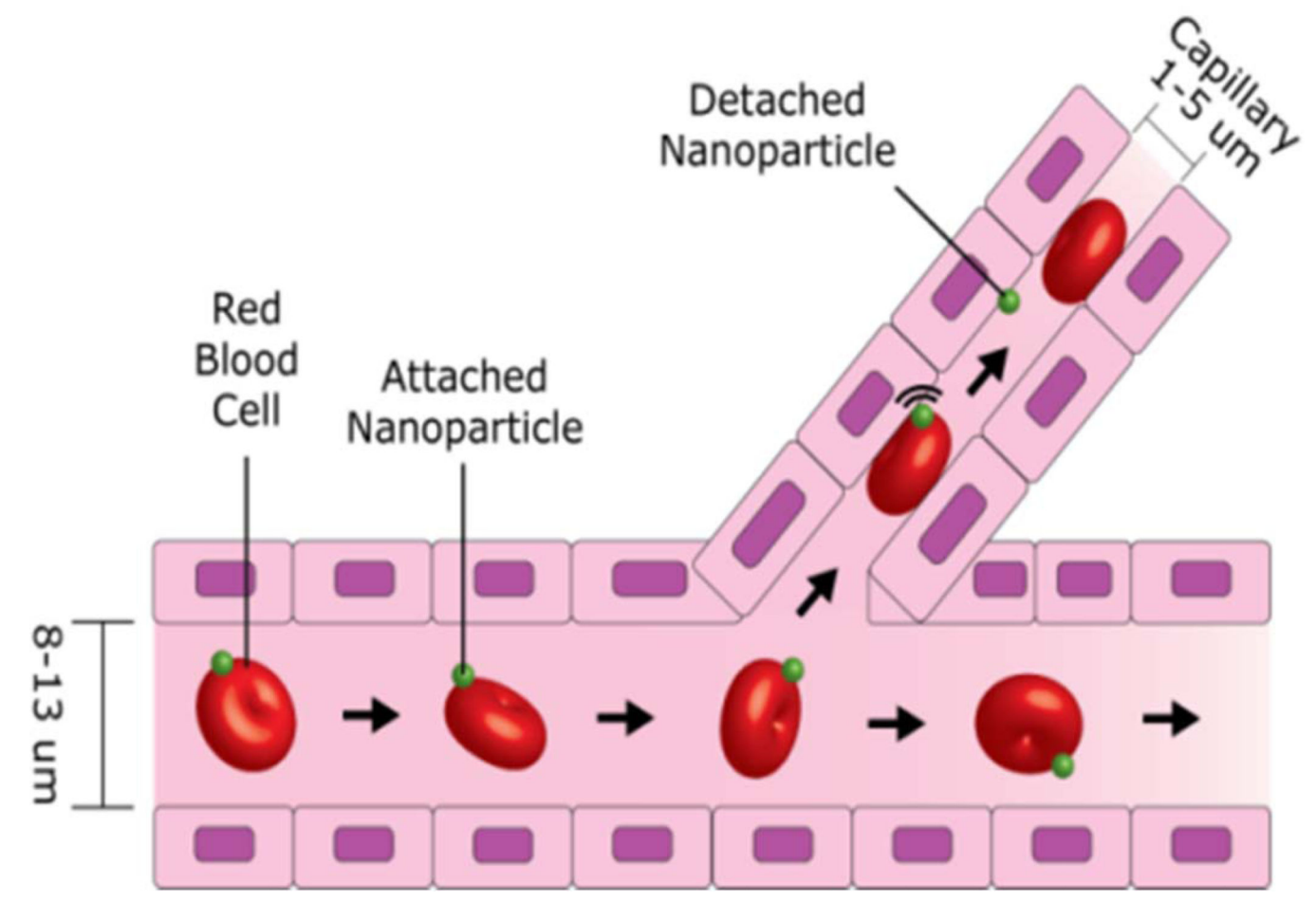


Figure 8. Schematic of particle detachment from RBCs in small capillaries

Schematic representing the detachment of NPs from RBCs in tiny capillaries present in lung microvasculature.